SERIES

Igneous Rock Associations 20. Pearce Element Ratio Diagrams: Linking Geochemical Data to Magmatic Processes

J. Nicholls[1] and J.K. Russell[2]

[1]Department of Geoscience
Earth Science 118
University of Calgary
2500 University Drive NW
Calgary, Alberta, T2N 1N4, Canada
Email: nichollj@ucalgary.ca

[2]Department of Earth, Ocean and Atmospheric Sciences
2020 - 2207 Main Mall
University of British Columbia
Vancouver, British Columbia, V6T 1Z4, Canada

SUMMARY

It has been nearly fifty years since Tom Pearce devised a type of element ratio diagram that isolates the effects of crystal fractionation and accumulation (sorting) hidden in the chemistry of a suite of igneous rocks. Here we review the guiding principles and methods supporting the Pearce element ratio paradigm and provide worked examples with data from the Mauna Ulu lava flows (erupted 1970–1971, Kilauea Volcano, Hawaii). Construction of Pearce element ratio diagrams requires minimum data; a single rock analysis can suffice. The remaining data test the model. If the data fit the model, then the model is accepted as a plausible or likely explanation for the observed chemical variations. If the data do not fit, the model is rejected. Successful applications of Pearce element ratios require the presence and identification of conserved elements; elements that remain in the melt during the processes causing the chemical diversity. Conserved elements are identified through a priori knowledge of the physical-chemical behaviour of the elements in rock-forming processes, plots of weight percentages of pairs of oxides against each other, or by constant ratios of two elements. Three kinds of Pearce element ratio diagrams comprise a model: conserved element, assemblage test, and phase discrimination diagrams. The axial ratios for Pearce ratio diagrams are combinations of elements chosen on the basis of the chemical stoichiometry embedded in the model. Matrix algebra, operating on mineral formulae and analyses, is used to calculate the axis ratios. Models are verified by substituting element numbers from mineral formulae into the ratios. Different intercepts of trends on Pearce element ratio diagrams distinguish different magma batches and, by inference, different melting events. We show that the Mauna Ulu magmas derive from two distinct batches, modified by sorting of olivine, clinopyroxene, plagioclase and, possibly, orthopyroxene (unobserved).

RÉSUMÉ

Il y a près de cinquante ans Tom Pearce a conçu un genre de diagramme de ratio d'éléments qui permet d'isoler les effets de la cristallisation fractionnée et de l'accumulation cristalline (tri) au sein de la chimie d'une suite de roches ignées. Dans le présent article, nous passons en revue les principes et les méthodes étayant le paradigme de ratio d'éléments de Pearce, et présentons des exemples pratiques à partir de données provenant de coulées de lave du Mauna Ulu (éruption 1970–1971 du volcan Kilauea, Hawaii). La confection des diagrammes de ratio d'éléments de Pearce requière un minimum de données; une seule analyse de roche peut suffire. Les données restantes servent à tester le modèle. Si les données sont conformes au modèle, alors le modèle est accepté comme explication plausible ou probable des variations chimiques observées. Si les données ne correspondent pas, le modèle est rejeté. Les applications réussies des ratios d'éléments de Pearce requièrent la présence et l'identification d'éléments conservés; éléments qui demeurent dans la masse fondue au cours des processus causant la diversité chimique. Les éléments con-

Geoscience Canada, v. 43, http://www.dx.doi.org/10.12789/geocanj.2016.43.095 pages 133–146
GC Data Repository: Igneous Rock Associations Series

servés sont identifiés par la connaissance a priori du comportement physico-chimique des éléments dans les processus de formation des roches, le positionnement sur la courbe des pourcentages pondérés de pairs d'oxydes les uns contre les autres, ou par des ratios constants de deux éléments. Trois types de diagrammes de Pearce de ratio d'éléments constituent un modèle: élément conservé, test d'assemblage, et diagrammes de phase discriminant. Les ratios axiaux pour les diagrammes de ratio d'éléments de Pearce sont des combinaisons d'éléments choisis sur la base de la stœchiométrie inhérente au modèle. L'algèbre matricielle, appliquée à des formules minérales et à des analyses, est utilisée pour calculer les ratios axiaux. Les modèles sont vérifiés en utilisant les nombres d'élément des formules minérales dans les ratios. Différentes intersections dans les diagrammes de ratios d'éléments de Pearce distinguent différents lots de magma et, par inférence, différentes coulées. Nous montrons que les magmas de Mauna Ulu proviennent de deux lots distincts, modifiés par l'extraction de l'olivine, de clinopyroxène, de plagioclase et, éventuellement, orthopyroxène (non observé).

Traduit par le Traducteur

INTRODUCTION

Pearce element ratios and diagrams are effective and efficient methods for extracting information on mineral accumulation and loss in magmas. Grounded in mineral stoichiometry, Pearce element ratios and diagrams faithfully depict the chemical variations in geochemical data sets collected from rocks in a volcanic field or from an intrusive suite. This article serves as a review, intended to demonstrate the power of the methods to recover igneous processes from geochemical data sets and to provide a blueprint for students to follow in order to apply the methods to their own rocks.

Pearce element ratios were first conceived by Pearce (1968) and subsequently further developed by Russell and Nicholls (1988), Oviatt and Nash (1989), Nicholls and Russell (1990), Russell et al. (1990), Russell and Stanley (1990a, b), Nicholls and Russell (1991), among many others. More recently, the concepts and methods developed by Pearce (1968) have been expanded and applied to altered rocks (Stanley 1993, 2003, 2006a, b) and to sulfide deposits (Beswick 2002, 2013).

Pearce element ratio diagrams are rectilinear plots featuring combinations of elements cast into ratios (Fig. 1). By definition, Pearce element ratios use a common element or combinations of elements in their denominators. That element in the denominator must be *conserved* (Nicholls 1988). A conserved element is any element essentially excluded from the differentiation processes; it remains sequestered in the melt. The effectiveness of Pearce element ratio diagrams derives from two main factors:

1. The geochemical data sets are converted to element ratios using a conserved element as the denominator of the ratios (Fig. 1). This transformation removes the effects of closure, rendering the resulting geochemical patterns as a direct and true record of the differentiation processes.
2. Differentiation involving igneous minerals, with their chemical stoichiometry, leaves an imprint on the associated melt compositions. Pearce element ratio diagrams are designed to compare the chemistry of model processes against the actual chemical variations recorded by the rock compositions.

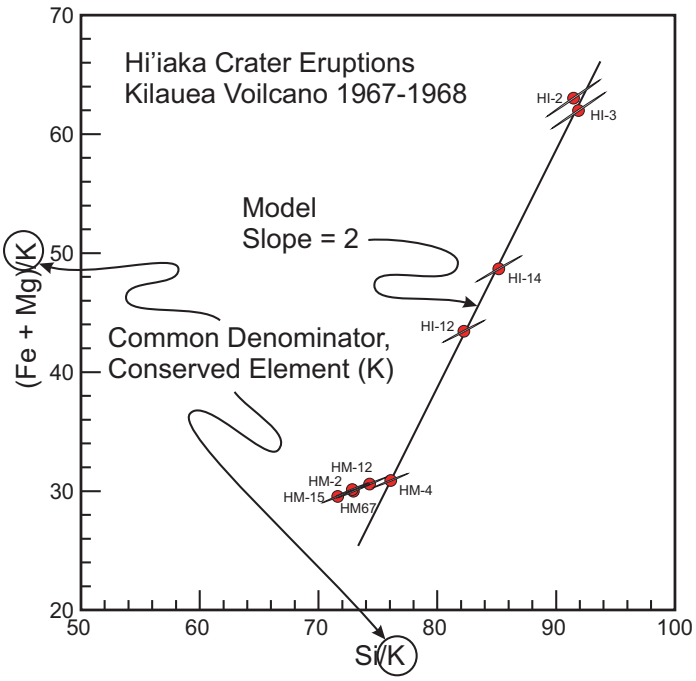

Figure 1. Pearce element ratio diagram and its parts. Plot of (Fe + Mg)/K versus Si/K. The model line has a slope of 2. If the data are related by the fractionation or accumulation of olivine, they should fall on a trend with a slope of 2. Five of the lava flows (HI02, HI03, HI14, HI12, and HM04) have compositions that supply ratios that fall close to the line. The other four samples (HM12, HM02, HM15, and HM67) fall on a trend with a slope less than two. Potassium is the conserved element and the intercept at X = 0 is off the graph.

For example, sorting (i.e. loss or gain) of olivine phenocrysts is a common explanation for the chemical diversity in basaltic melts. Furthermore, K represents an element that is expected to be conserved throughout basaltic differentiation. Because ideal stoichiometric olivine contains two Mg + Fe atoms for every Si atom, a plot of (Mg + Fe)/K versus Si/K on a Pearce element ratio diagram prescribes a slope of 2 for the model. The Pearce element diagram (Fig. 1) allows for an easy graphical comparison of the model line to the distribution of real data. Figure 1 displays the graphical implications of olivine loss or accumulation in a suite of co-magmatic olivine-rich basaltic lava flows erupted at Hi'iaka Crater, Kilauea in 1968. Several of the ratio values plot on (or very near) the line with a slope of 2 and are fully explained by sorting of olivine phenocrysts; several data points do not, however, and these data points require a different model to explain the chemical variations.

The values of the ratios, the number pairs (X, Y) (Russell and Nicholls 1988), that plot on a Pearce element ratio diagram come from a rock analysis. The weight percent of the constituent in the analysis that contains the element in question is divided by the formula weight of the constituent and multiplied by the number of elements in the constituent. These numbers are then used to calculate the X- and Y-values for the ratios. The same procedure is followed for each analysis in the data set. The simple element ratios for the rock analyses listed in Table 1 are set down in Table 2.

Here, our goals are three-fold. 1) To provide a review of the basic Pearce element ratio paradigm which comprises three main types of diagrams: i) conserved element diagrams, ii) assemblage test diagrams, and iii) phase discrimination diagrams. 2) To provide detailed instructions on how to design Pearce element ratio diagrams to explore or test specific processes or models. These simple matrix operations allow readers to develop their own diagrams to address their specific situations. 3) To describe the importance of the intercept in Pearce element ratio diagrams as they provide a way to discriminate between individual magma batches and, by inference, melting events.

We will demonstrate features of Pearce element ratios and diagrams using data collected on lava flows from the 1970–1971 Mauna Ulu eruptions from Kilauea Volcano, Hawaii. The samples come from lava flows erupted from 9 April, 1970 through 19 April, 1971 (Wright et al. 1975). The trace element data are from Hofmann et al. (1984). The data are listed in Table 1 for those wanting to calculate their own diagrams.

Table 1. Oxide (wt. %) and trace element (ppm) concentrations for the Mauna Ulu lava flows from Wright et al. (1975) and Hofmann et al. (1984), respectively.

Oxide	70-25	70-35	70-41	70-62	70-83	71-127	71-134	71-136	71-137
SiO_2	49.91	49.51	49.74	49.14	49.43	49.38	50.48	49.73	49.16
TiO_2	2.44	2.30	2.38	2.15	2.21	2.13	2.31	2.21	2.10
Al_2O_3	13.52	13.00	13.14	12.18	12.63	12.48	13.63	12.91	12.20
Fe_2O_3	1.39	1.08	1.07	1.15	1.13	1.16	1.27	1.20	1.16
FeO	10.07	10.53	10.44	10.62	10.57	10.54	10.06	10.37	10.67
MnO	0.18	0.18	0.17	0.17	0.17	0.18	0.17	0.18	0.18
MgO	8.55	10.01	9.57	12.02	10.92	11.33	8.14	10.33	11.96
CaO	10.85	10.41	10.60	9.86	10.19	10.06	11.05	10.31	9.85
Na_2O	2.27	2.21	2.20	1.98	2.11	2.02	2.22	2.10	2.20
K_2O	0.47	0.41	0.43	0.40	0.40	0.39	0.41	0.40	0.37
P_2O_5	0.23	0.21	0.23	0.21	0.22	0.21	0.22	0.21	0.20
Total	99.88	99.85	99.97	99.88	99.98	99.88	99.96	99.95	100.05
Trace elements									
Ce	32.60	30.70	31.10	28.50	29.20	27.90	30.30	28.00	27.20
Nd	21.20	19.90	20.10	18.40	19.00	18.30	19.60	18.60	17.60
Sm	5.43	5.19	5.21	4.75	4.96	4.76	5.16	4.83	4.64
Eu	1.84	1.79	1.80	1.65	1.71	1.66	1.80	1.68	1.64
Dy	5.01	4.78	4.83	4.45	4.62	4.54	4.94	4.65	4.42
Er	2.45	2.37	2.38	2.20	2.26	2.25	2.49	2.31	2.22
Yb	1.95	1.86	1.90	1.75	1.77	1.81	2.04	1.85	1.79

Table 2. Single element ratios calculated for the analyses reported in Table 1.

Ratio	70-25	70-35	70-41	70-62	70-83	71-127	71-134	71-136	71-137
Si/K	83.240	94.657	90.673	96.298	96.866	99.249	96.511	97.454	104.148
Ti/K	3.060	3.307	3.263	3.168	3.257	3.219	3.321	3.257	3.346
Al/K	26.575	29.293	28.231	28.131	29.170	29.563	30.712	29.817	30.462
Fe/K	15.970	18.606	17.588	19.323	19.211	19.698	18.118	18.982	20.996
Mn/K	0.254	0.291	0.262	0.282	0.282	0.306	0.275	0.299	0.323
Mg/K	21.258	28.530	26.007	35.115	31.902	33.948	23.200	30.178	37.773
Ca/K	19.388	21.324	20.703	20.702	21.395	21.664	22.635	21.647	22.358
Na/K	7.340	8.192	7.776	7.523	8.017	7.872	8.229	7.979	9.037
P/K	0.325	0.340	0.355	0.348	0.365	0.357	0.356	0.348	0.359

CONSERVED ELEMENT SELECTION

Trends on a Pearce element ratio diagram will be petrologically significant only if the common denominator is conserved during the physical-chemical processes that produced the chemical variations in the data. The first task is to determine whether a conserved element exists in the data set. There are three ways to do this.

1. Our a priori knowledge of the physical-chemical behaviour of the elements in rock-forming systems may suggest conserved element status. This criterion, knowledge of the physical-chemical behaviour, is probably the most important one. Unless an element is likely to be conserved, there is no point in using that element as the common denominator to the Pearce element ratios. For example, in most igneous rocks, P is expelled from the melt only in the late stages of crystallization when apatite forms. In volcanic rocks, apatite almost always occurs as tiny, unnoticeable crystals in the groundmass. In plutonic rocks, apatite often occurs as scattered, small subhedral to euhedral crystals, too small to be fractionated in silica-rich melts. Consequently, the physical-chemical behaviour of P in igneous systems suggests that it is likely a conserved element.
2. A plot of the weight percentages of pairs of oxides against each other will define a single linear trend having a zero intercept if the elements in the oxides are conserved (Stanley and Madeisky 1995; see Fig. 2A, B, C). Figure 2D shows the contrasting case where the oxides of two non-conserved elements are plotted against each other. The data plotted on Figure 2 come from the 1970–1971 Mauna Ulu lava flows (Table 1).
3. The ratio of two conserved elements (e.g. P/K) should be constant. Constant ratios indicate that both elements are conserved constituents; only by chance can the ratios be constant and the elements not conserved. The variations in the ratios of these elements within a single data set should not be significantly greater than the variation that can be attributed to analytical uncertainty. Figure 3 plots Ti/K vs. P/K for the Mauna Ulu eruptive products. If all 3 elements are equally conserved, and the 1970 and 1971 lava flows derive from a single chemical system, the entire geochemical data set should plot in a single cluster (see below and Fig. 3A). The dispersion in the data around the mean value should not be larger than can be explained by analytical error.

TYPES OF PEARCE ELEMENT DIAGRAMS

Several models have been put forward to explain the diversity found in the Mauna Ulu magmas. Crystal sorting, magma mix-

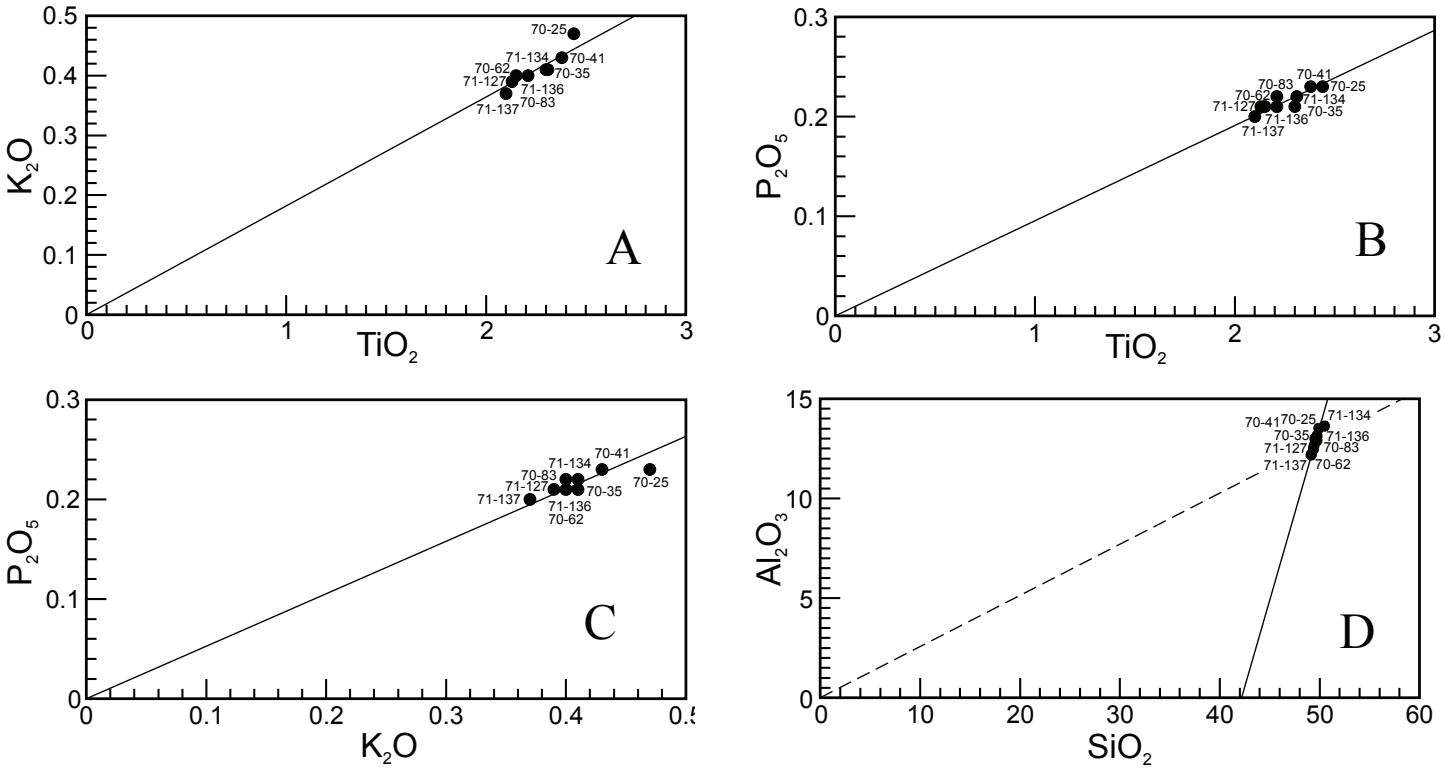

Figure 2. An empirical method for discovering conserved elements (Stanley and Madeisky 1995). Weight percentages of oxides containing potential conserved elements plotted against each other. Data for the Mauna Ulu 1970–1971 lava flows. (A) K_2O–TiO_2, (B) P_2O_5–TiO_2, (C) P_2O_5–K_2O. If the elements are potentially conserved they will fall along a trend through the origin. (D) Contrasting behaviour for elements that are not conserved. The latter fall on a line that does not pass through the origin (solid line).

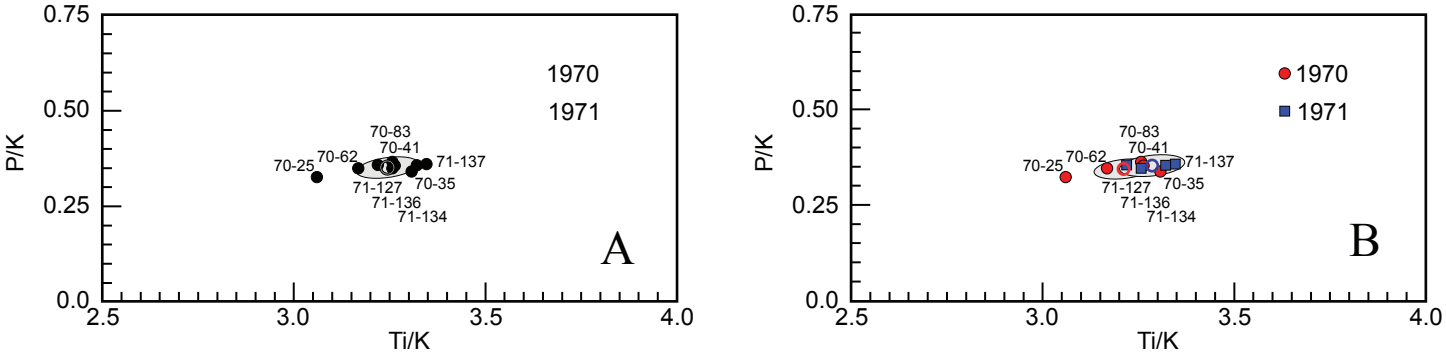

Figure 3. Conserved element plots for the 1970–1971 Mauna Ulu lava flows. Plotted are two ratios formed from three elements likely to be conserved in basaltic systems: P/K and Ti/K. Mean values are indicated by open circles. The shaded ellipses represent the expected variation in location of the mean values due to analytical uncertainty. (A) Distribution of the data points for the entire 1970–1971 data set. Several points fall outside the expected uncertainty about the mean, especially along the Ti/K axis. (B) Distribution of data points grouped by date of eruption. The 1971 data points fall within their uncertainty ellipse, whereas two of the 1970 data points (70-25 and 70-35) do not.

ing, and compositional variations in the source regions of the magmas have been invoked, either singly or in combination, as models (see Hofmann et al. 1984 and Vinet and Higgins 2010, for further description and discussion). Pearce element ratio diagrams can help discriminate between these competing ideas.

Conserved Element Diagrams

We begin with conserved element diagrams because they provide information about consanguinity of magmas. The 1970–1971 Mauna Ulu lava flows are basalt made of olivine, plagioclase, augite, opaque minerals, and variable amounts of glass. The bulk composition of the Mauna Ulu magma, the mineral assemblage, and the typical physical-chemical behaviour of the mineral phases leads us to expect that at least three elements could be conserved: Ti, K, and P. In our analysis of the Mauna Ulu data we will use K as the conserved element. The propagated analytical uncertainties (Nicholls 1990; Halleran and Russell 1990) depend on the analytical method and the concentration of the substance. Usually K_2O has a higher concentration than P_2O_5 and a smaller uncertainty, making it the preferred denominator.

The remarkable feature of Figure 3A is the near uniformity in P/K values compared to Ti/K. The variation or scatter in P/K ratios for the combined data from both the 1970 and 1971 lava flows is explicable by analytical uncertainty alone. However, the range in Ti/K values exceeds that expected from analytical uncertainty (grey ellipse, Fig. 3A). If the data are segregated by time of eruption (Fig. 3B, 1970 versus 1971 data),

the data points more closely conform to the dispersion about the mean expected from analytical uncertainty. The P/K and Ti/K data points for the 1971 Mauna Ulu samples are enclosed by the analytical uncertainty ellipse centred on the mean value (open circle). However, the 1970 data set shows greater dispersion in Ti/K values and two data points (70-25 and 70-35) fall outside the corresponding ellipse (Fig. 3B). The dispersion in Ti/K values suggests minor sorting of a Ti-bearing phase, likely a Fe-Ti oxide. Obviously, we must consider models that distinguish between the two populations.

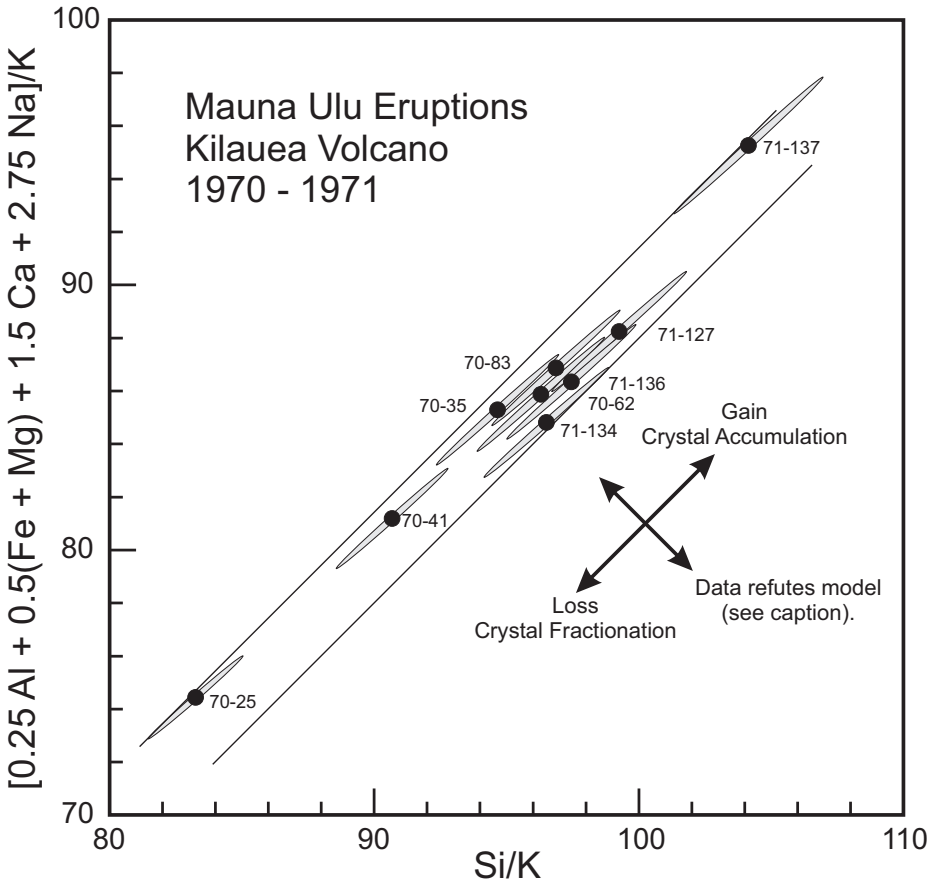

Figure 4. Assemblage test diagram to determine whether the chemical variations in the 1970–1971 lava flows from Kilauea Volcano, Hawaii, can be explained by sorting olivine, clinopyroxene, and plagioclase. The two lines with slopes of one straddle the data. The shaded ellipses represent the expected variation in location of the data points due to analytical uncertainty. The arrows show how data points should be distributed if one particular process dominates. Scatter away from a line with a slope of one caused by processes or factors not considered in the model design, such as multiple source compositions, magma mixing, non-conserved element in the denominator, gain or loss of a phase not included in the model.

Assemblage Test Diagrams

A first and logical model to explain the geochemical diversity in the Mauna Ulu lava flows is sorting of the phenocrysts typically found in basalt: olivine, augite, and plagioclase.

The Pearce element ratio diagram (Fig. 4) uses combinations of elements on the two axes to represent the proposed model. Specifically, the coefficients for the elements are chosen to exactly mimic the stoichiometric effects of sorting of the proposed mineral assemblage comprising any modal combination of olivine, clinopyroxene and plagioclase. This type of Pearce element ratio diagram is termed an Assemblage Test diagram (Stanley and Russell 1989, 1990); the methods used to find these effective, but non-intuitive, coefficients are discussed in detail below. The coordinates of the Mauna Ulu data points plotted in Figure 4 are listed in Table 3. For the moment we simply use the diagram to explore the chemical diversity of the Mauna Ulu lava flows.

Figure 4 is constructed such that lava flows from a single batch of basaltic magma that record the effects of differentiation by sorting combinations of olivine, clinopyroxene, and plagioclase will define a single straight line having a slope of one and, ideally, a non-zero intercept. Data seldom fit models perfectly but if the model is adequate, we expect the compositions of the lava flows to plot within analytical uncertainty of a single model line with unit slope. The ellipses on Figure 4 illustrate the analytical uncertainty that can be ascribed to each data point.

Data points representing rocks with accumulated minerals will plot on the model line at higher ratio values. Data points representing rocks that have fractionated (lost) minerals will plot on the model line at lower ratio values. Data points that scatter off the model line represent rocks related in other ways (Fig. 4).

What is absolutely clear is that the combined 1970–1971 Mauna Ulu data set (Figs. 1, 4) does not conform to a single straight line of any slope (compare Fig. 4 with Fig. 1) let alone a slope of one. Nor will two model lines with slopes of one fit the 1970 and 1971 Mauna Ulu compositions separately. Consequently, the differentiation model as stated above is inadequate; sorting of olivine, clinopyroxene, and plagioclase fails to explain all the chemical variations. Rather, some other or additional processes must play a role and this fact has led to the myriad of alternate explanations in the literature on Mauna Ulu magmas (see Hofmann et al. 1984; Vinet and Higgins 2010).

Trace element ratios provide insight into other processes that can contribute to, or limit, the chemical diversity of the Mauna Ulu magmas. Although partition coefficients control trace element concentration instead of mineral stoichiometry, ratios of trace elements can be integrated into Pearce element ratio diagrams (Halleran and Russell 1990; Russell and Halleran 1990). Figure 5 shows the ratio of two incompatible elements, Yb and Ce, projected onto the assemblage test diagram of Figure 4. The trace element data define two chemically distinct groups: (1) the 1970 flows (70-25, 70-41, 70-35, 70-62, and 70-83), and (2) the 1971 flows (71-127, 71-134, 71-136, and 71-137); evidence consistent with a model encompassing two separate chemical systems.

Analogous plots of ratios for the rare earth elements Er/Ce, Dy/Ce, Eu/Ce, Sm/Ce, and Nd/Ce are shown on Figure 6. With two exceptions, the REE data are consistent with two magma batches in the 1970–1971 data. The Nd/Ce ratios for 71-134 and 71-137 fail to fall at higher values than the high-

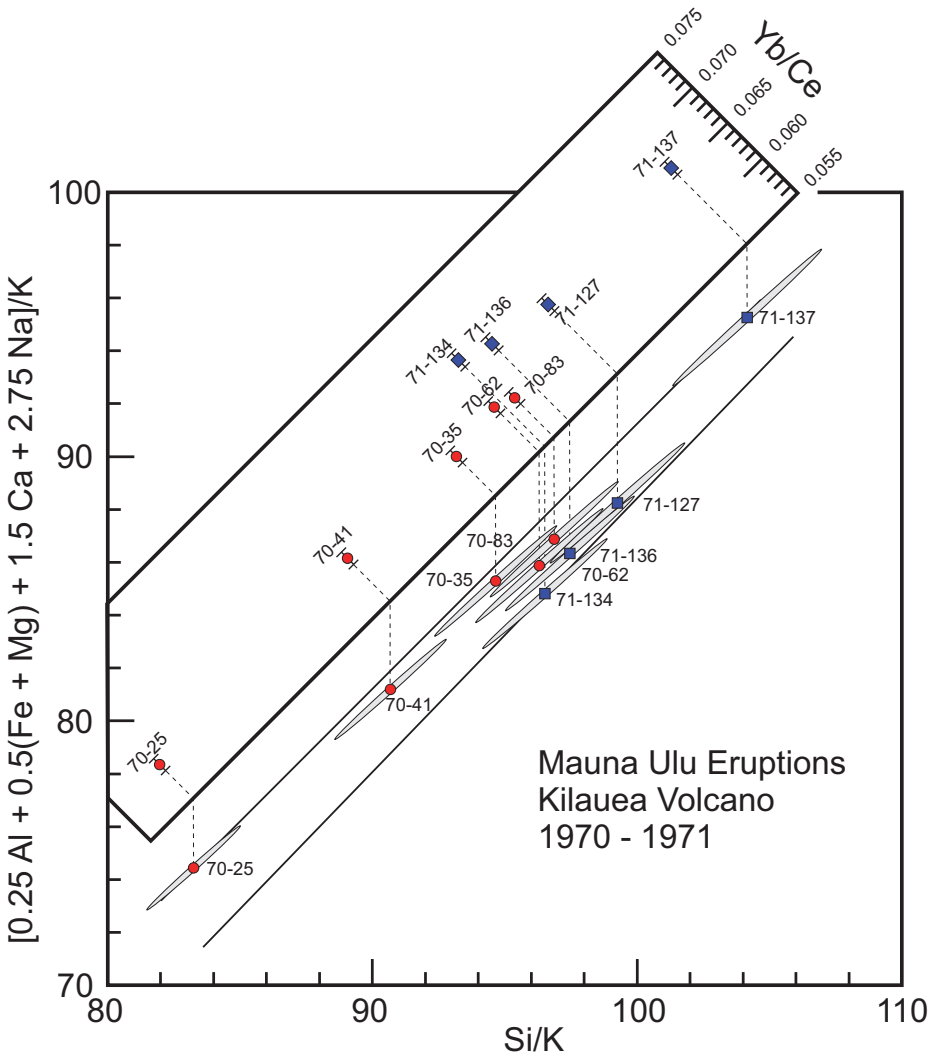

Figure 5. Same diagram as Figure 4 but with the ratios of two incompatible trace elements (Yb and Ce) projected on the diagram. The distribution of the trace element ratios distinguishes the flows erupted in 1970 from those erupted in 1971, indicating the presence of two chemical systems among the eruptive products. The shaded ellipses represent the expected variation in location of the data points due to analytical uncertainty.

est values of the 1970 ratios although some are within our estimates of analytical uncertainty.

Phase Discrimination Diagrams

The 1970–1971 Mauna Ulu lava flows belong to two distinct chemical systems, one represented in the 1970 lava flows and the other in the 1971 lava flows (Figs. 4, 5). The assemblage test diagram designed to test a model of sorting of olivine, clinopyroxene, and plagioclase in any combination, showed that the chemical variations within and between the two lava groups are inconsistent with simple sorting of the common basalt phenocryst assemblage. Furthermore, the ratios of most of the rare earth elements are distinct and coherent for the 1970 versus 1971 Mauna Ulu lava flows (Figs. 5, 6). This precludes simple mixing of the two chemical systems as an explanation for the diversity.

What other possibilities make physical-chemical sense? The natural choice is to add another phase to the sorted assemblage. An Fe-Ti oxide and/or orthopyroxene crystallize in many basaltic magmas and are likely candidates.

The conserved element ratio diagram (Fig. 3) suggests Ti is not conserved in all the samples, especially sample number 70-25. An assemblage test diagram that incorporates the possibility of an Fe-Ti oxide having a composition equal to 75% ulvospinel, 25% magnetite is shown on Figure 7. Four of the five 1970 data points fall close to a line with a slope of one (70-41, 70-35, 70-62, and 70-83). 70-25, however, falls more than one unit of analytical uncertainty from the line. None of the 1971 data points fall on the same line with its slope of one nor do they fall on a different line with a slope of one. Sorting of an Fe-Ti oxide may be a factor in creating chemical diversity in the 1970 data but it is an incomplete explanation at best. It fails to explain the scatter in the 1971 data.

Orthopyroxene (or another low-calcium pyroxene, e.g. pigeonite) occurs in the phenocryst assemblages of some basaltic rocks along with plagioclase, olivine, and clinopyroxene (Deer et al. 2013). Below, we give reasons for including orthopyroxene in the sorted assemblage that go beyond the simple fact that it is found in some basalt suites. Here, our purpose is to introduce another type of Pearce element ratio diagram, the phase discrimination diagram. This diagram isolates the effects a rival phase would have on a trend caused by sorting. Orthopyroxene will be the rival phase. The coefficients of such diagrams are designed to force the greatest deviation from a line with slope of one if sorting of the rival phase occurs (Stanley and Russell 1989, 1990). Again, the methods for the calculation of the coefficients are discussed below. The phase discrimination diagram shown in Figure 8 is designed to test the model of sorting of olivine ± clinopyroxene ± plagioclase, but has the property such that sorting of orthopyroxene will have a maximum discernible effect; orthopyroxene sorting causes a trend to develop at right angles to the trend caused by sorting of the other phases.

In this phase discrimination diagram (Fig. 8), the Mauna Ulu data show increased scatter compared to Figures 4, 5, and 7. The nature of the scatter is consistent with orthopyroxene sorting contributing to the chemical variations within the data sets. The 1970 Mauna Ulu lava flows could have fractionated orthopyroxene with the other three phases; this conclusion follows from the data defining a trend with a slope greater than one. Orthopyroxene accumulation accompanied by fractionation of the other three phases is suggested by the trend defined by the 1971 data where the slope of the trend is less than one. However, in both cases, the total chemical effect of orthopyroxene sorting is subordinate to the effects of sorting of olivine ± clinopyroxene ± plagioclase. The slopes of the lines through the trends (Fig. 8) lead to estimates of 0.15–0.25 for the ratios of orthopyroxene to olivine ± clinopyroxene ± plagioclase in the sorted assemblages.

Table 3. Element ratios for the 1970–1971 Mauna Ulu eruptions as plotted on Figures 6 and 7 with X = Si/K and Y = [0.25 Al + 0.5 (Fe + Mg) + 1.5 Ca + 2.75 Na]/K. Also listed are the Y-intercepts for lines drawn through each data point (Y_0) and having a model slope of 1.0 and the corresponding mean values, the standard deviations (s) and the analytical uncertainty associated with the data set and subsets (s_A).

Sample	X-axis Ratio	Y-axis Ratio	Intercept (Y_0)
70-25	83.24	74.435	-8.804
70-41	90.673	81.191	-9.482
70-35	94.657	85.297	-9.359
70-62	96.298	85.882	-10.416
70-83	96.866	86.877	-9.989
71-134	96.511	84.817	-11.694
71-136	97.454	86.338	-11.116
71-127	99.249	88.243	-11.006
71-137	104.148	95.267	-8.882
Mean	95.455	85.372	-10.083
s	5.8147	5.5568	1.0367
s_A	4.7362	4.2512	0.7072
70- Mean	92.347	82.736	-9.61
70- s	5.6371	5.121	0.6169
70- s_A	4.4348	3.9857	0.5696
71- Mean	99.341	88.666	-10.675
71- s	3.4003	4.6183	1.2325
71- s_A	5.0879	4.5613	0.6512

DESIGNING DIAGRAMS WITH LINEAR ALGEBRA

So, how does one calculate the complex, non-intuitive, elemental coefficients used in the assemblage test and phase discrimination diagrams (i.e. Figs. 4, 5, 7, 8)? The challenge is to find combinations of ratios for the axes of the Pearce element ratio diagram that will cause the geochemical data points to plot as a line with a prescribed slope. The slope of the line is prescribed by the model and by the mineral stoichiometry of the sorted phases. The expectation that the data points will fall on the line is a consequence of the model. The slope most commonly prescribed is one.

Matrix algebra provides the most efficient methods for determining the ratios and the methods are straight-forward if the slope is one. Stanley and Russell (1989, 1990), and Nicholls and Gordon (1994) provide extensive descriptions of the requisite matrix methods.

Two types of matrix equations are used to derive the ratios for a Pearce element ratio diagram that tests the consequences of a model: assemblage test equations and phase discrimination equations (Stanley and Russell 1990). As used above in our analysis of the 1970–1971 Mauna Ulu lava flows, assemblage test diagrams are used to determine whether the variations in the data can be explained by sorting of an assemblage of one or more phases, whereas phase discrimination diagrams are used to determine whether a particular phase is required to explain the variations in the data.

Designing Assemblage Test Diagrams

The starting point is a matrix equation that can be written:

$$\mathbf{C \cdot A = P} \qquad \textit{(Eq. 1)}$$

where **C** is the (M x N) matrix of the compositions of the phases causing differentiation. M is the number of phases in the system (for example, M = 4 for the assemblage olivine, albite, anorthite, and clinopyroxene). N is the number of distinct elements in the phases being sorted (N = 5 in our example: Si, Al, Fe + Mg, Ca, and N). The rows of **C** are the compositions of the phases and the columns are the elements in each phase. These numbers come from the mineral formulae of the phases we think caused the chemical variations.

A is an (N x 2) matrix of unknown coefficients of the elements that appear in the numerators of the ratios. The two columns are themselves matrix vectors, **X** and **Y**. **X** contains the coefficients of the elements in the numerator of the ratio plotted on the X-axis and **Y** contains the coefficients for the other axis ratio. The components of **X** and **Y** are the unknowns we want to find by solving the matrix equation (Eq. 1).

The column vectors of matrix **P**, which is an M x 2 matrix, are the displacement vectors: **u** and **v**. The M rows of **P** (i.e. the mathematical elements of **u** and **v**) are the relative displacement vectors for each of the M minerals on the two axes of the Pearce element ratio diagram. The relative displacement vectors are set by the slope of the line we choose to assign to the hypothesis. If we want a slope of 1 for each of the M minerals involved in a sorting hypothesis, then the corresponding row elements of **u** and **v** for each phase will be set equal (e.g. $u_i = v_i$). If for some reason a slope of 2 were preferred then all row elements would be adjusted accordingly: $u_i = 0.5\ v_i$, where v_i is an arbitrary number. The magnitude of v_i chosen dictates the length of the resulting displacement vector for each model phase; it is common to set v_i to 1.0 so each phase will have the same relative displacement on the Pearce element ratio diagram.

For the assemblage: plagioclase, olivine, clinopyroxene, the matrix equation, (Eq. 1), can be written:

$$\begin{array}{c} \mathbf{C} \\ \begin{array}{c} \text{Si Al FM Ca Na} \\ \begin{array}{l}\text{An}\\ \text{Ab}\\ \text{Ol}\\ \text{Cp}\end{array} \begin{bmatrix} 2&2&0&1&0\\ 3&1&0&0&1\\ 1&0&2&0&0\\ 2&0&1&1&0 \end{bmatrix} \end{array} \end{array} \begin{array}{c} \mathbf{A} \\ \begin{bmatrix} x_1 & y_1\\ x_2 & y_2\\ x_3 & y_3\\ x_4 & y_4\\ x_5 & y_5 \end{bmatrix} \end{array} = \begin{array}{c} \mathbf{P} \\ \begin{bmatrix} u_1 & v_1\\ u_2 & v_2\\ u_3 & v_3\\ u_4 & v_4 \end{bmatrix} \end{array} \qquad \textit{(Eq. 2)}$$

Because the two matrices, **A** and **P**, each consist of two column vectors, the last equation (Eq. 2) can be split into two:

$$\mathbf{C \cdot X = u} \qquad \textit{(Eq. 3)}$$
$$\mathbf{C \cdot Y = v} \qquad \textit{(Eq. 4)}$$

If the desired slopes for all the phases represented by the displacement vectors are 1, then the constraints on the slopes, as reflected in the displacement vectors, **u** and **v**, can be written:

$$\mathbf{u = v} \qquad \textit{(Eq. 5)}$$

or for each i, $u_i = v_i = 1$.

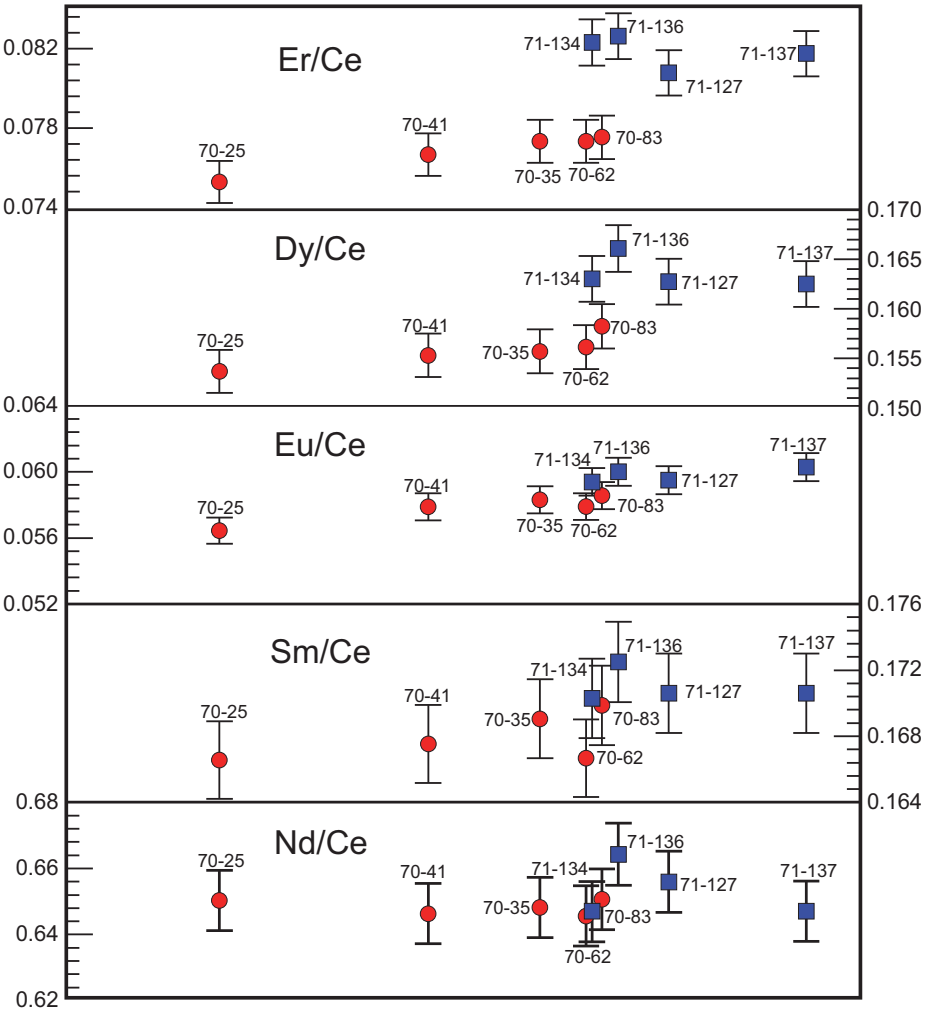

Figure 6. Rare earth element ratios for the 1970–1971 Mauna Ulu lava flows. The horizontal scale is the same as that shown on Figure 7 for Yb/Ce.

For a slope of one, the displacement along the X-axis must equal the displacement along the Y-axis.

Hence:

$$\mathbf{C} \cdot (\mathbf{X} - \mathbf{Y}) = \mathbf{0} \qquad \textit{(Eq. 6)}$$

If the number of phases, *M*, is less than the number of elements in the phases, *N*, then the rank of **C** must be less than *N* and there may be a non-trivial solution to Equation 6 (i.e. a useful set of coefficients). The solution vectors of Equation 6 can be obtained by various methods, such as singular value decomposition, outlined in matrix algebra texts (Press et al. 1992) or by successive row operations. A calculator for doing the latter process can be found on-line at: www.math.purdue.edu/~dvb/matrix.html. The elements of the solution vector can be normalized, if desired, so that the coefficient of at least one of the chemical elements in the numerator of the X-axis ratio, say, is equal to one.

If the conserved element is K, the ratio pair derived by solving Equation 2 – Equation 6 is:

[0.25 Al + 0.5 (Fe + Mg) + 1.5 Ca + 2.75 Na]/K versus Si/K *(Eq. 7)*

and:

Al/K versus (2 Ca + Na)/K *(Eq. 10)*

A given model may lead to more than one set of coefficients and more than one Pearce element ratio diagram will provide additional tests. In fact, the number of valid Pearce element ratio diagrams that can be derived from a matrix of phase compositions, **C**, is equal to the column size of the matrix, *N*, minus the rank of the matrix, a number called the nullity of the matrix (Ayres 1962). In the example above (Eq. 4), the column dimension of the matrix **C** is five and its rank is four; thus, there is a single solution.

Suppose, however, that the hypothesis called for only three phases or end members: albite, anorthite, and olivine. The system of equations then becomes:

$$\underset{\text{Si Al FM Ca Na}}{\mathbf{C}} \quad \mathbf{A} \quad \mathbf{P}$$

$$\begin{matrix} \text{An} \\ \text{Ab} \\ \text{Ol} \end{matrix} \begin{bmatrix} 2 & 2 & 0 & 1 & 0 \\ 3 & 1 & 0 & 0 & 1 \\ 1 & 0 & 2 & 0 & 0 \end{bmatrix} \begin{bmatrix} x_1 & y_1 \\ x_2 & y_2 \\ x_3 & y_3 \\ x_4 & y_4 \\ x_5 & y_5 \end{bmatrix} = \begin{bmatrix} u_1 & v_1 \\ u_2 & v_2 \\ u_3 & v_3 \end{bmatrix} \qquad \textit{(Eq. 8)}$$

an equation for which the number of columns (5) minus the number of rows (3) equals 2, indicating that there are two Pearce element ratio diagrams that can test the same model against the data. The solutions to Equation 8 can be cast into the ratios that we plot on the X-axis and Y-axis.

(Si + 0.333 Ca)/K versus
[1.167 Al + 0.5(Fe + Mg) + 1.833 Na]/K *(Eq. 9)*

In vector form, the two solutions to the matrix equation (Eq. 8) are:

	$(\mathbf{X}-\mathbf{Y})_1$	$(\mathbf{X}-\mathbf{Y})_2$
Si	1.0	0.0
Al	-1.167	1.0
Fm	-0.5	0.0
Ca	0.333	-2.0
Na	-1.833	-1.0

We arbitrarily assign positive values in the solutions to coefficients of elements in the numerator of the ratio plotted on the X-axis whereas negative values, with the minus sign dropped, are assigned to coefficients in the numerator of the ratio plotted on the Y-axis.

Generally, if the number of phases, *M*, is equal to the number of elements, *N*, the rank of **C** will also equal *N*. In such instances, the set of homogeneous equations:

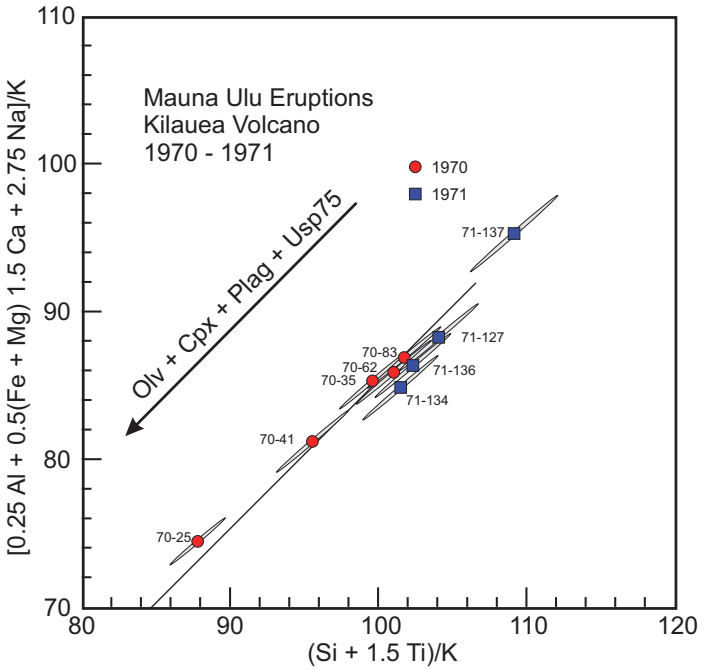

Figure 7. Assemblage test diagram to determine if a model with sorting of olivine, clinopyroxene, plagioclase, and a Fe-Ti oxide (Usp75) accounts for the distribution of the data points (compare Fig. 5). The shaded ellipses represent the expected variation in location of the data points due to analytical uncertainty. The solid line with a slope of one line touches all the 1970 error ellipses except 70-25.

$$\mathbf{C} \bullet (\mathbf{X} - \mathbf{Y}) = \mathbf{0} \qquad \textit{(Eq. 11)}$$

will only have the trivial solution $(\mathbf{X} - \mathbf{Y}) = \mathbf{0}$ or, in other words, the X-axis ratio is the same as the Y-axis ratio. This will produce a plot with a perfect straight line but it will also contain no information. Exceptions to this point occur if the rank of the coefficient matrix is less than *N*. If the composition of one (or more) of the phases is a linear combination of some of the other phases, then the rank of **C** will be less than *N*.

Suppose, for example, the hypothesis is that the variations are due to sorting of plagioclase, clinopyroxene, olivine, ulvospinel and apatite. The number of phases or end members, *M*, is 8: An, Ab, Fo, Fa, Di, Hd, Up, and Ap. The number of elements to be placed in the ratios, *N*, is also 8: Si, Al, Ti, Fe, Mg, Ca, Na, and P. The rank of the coefficient matrix, **C**, is less than 8 because there is a linear combination relating the compositions of four of the end members, fayalite, diopside, hedenbergite, and forsterite:

$$\tfrac{1}{2}\ Fe_2SiO_4 + CaMgSi_2O_6 = CaFeSi_2O_6 + \tfrac{1}{2}\ Mg_2SiO_4 \qquad \textit{(Eq. 12)}$$

A pair of ratios that will provide a slope of one on a Pearce element ratio diagram, if the variations are due to sorting of plagioclase, clinopyroxene, olivine, ulvospinel, and apatite are:

$$\frac{(2.25\ Al + 0.5\ FM\ 1.5\ Ca + 2.75\ Na)}{K} \text{ versus } \frac{(Si + Ti + 2.5\ P)}{K} \qquad \textit{(Eq. 13)}$$

Assemblage test diagrams need not have axial ratios defining a slope of one if sorting of the model assemblage produced the chemical variations. The matrix equation, Equation 1, however, reduces to a system of homogeneous equations, Equation 7, only if the model slope is equal to one.

Designing Phase Discrimination Diagrams

In our analysis of the geochemical diversity of the 1970–1971 Mauna Ulu lava flows, we considered whether or not orthopyroxene may have been involved in the differentiation process. To test this model, we designed a phase discrimination diagram (Fig. 8) to test for potential sorting of the rival phase, orthopyroxene $[(Mg,Fe)_2Si_2O_6]$, versus sorting only of olivine, clinopyroxene, and plagioclase.

For this rival phase we want the displacement vectors to point in a direction at a high angle (i.e. perpendicular) to the model trend, which usually has a slope of 1. As a result, the right side of Equation 6 will not be a zero vector and the system of equations will not be homogeneous.

The components of the displacement vectors for orthopyroxene (Op) must be such that the orthopyroxene vector has a slope of –1 on a Pearce element diagram. Such a feature will occur if $\mathbf{u}_{Op} = -\mathbf{v}_{Op}$.

If we assign the coefficients of the elements in the numerator of the left-ratio to **X** and the coefficients of the elements in the numerator of the right ratio (Eq. 8) to **Y**, then one can show that the resulting vectors satisfy the equation:

$$\mathbf{C} \bullet (\mathbf{X} - \mathbf{Y}) = \mathbf{0} \qquad \textit{(Eq. 14)}$$

Note that the components of the column vectors corresponding to orthopyroxene have opposite signs.

Again, because of equality in number of elements in the vectors **X** and **Y** and in the vectors **u** and **v**, this last equation can be written as two:

$$\mathbf{C} \bullet \mathbf{X} = \mathbf{u} \qquad \textit{(Eq. 15)}$$
$$\mathbf{C} \bullet \mathbf{Y} = \mathbf{v} \qquad \textit{(Eq. 16)}$$

The coefficients for the **X** and **Y** vectors for these non-homogeneous systems of equations can be extracted by solving for **X** and **Y** separately. Solving Equation 15 will provide the coefficients for the numerator of the ratio plotted on the X-axis, whereas solving Equation 16 provides the coefficients for the numerator of the ratio plotted on the Y-axis. These two equations are, in general, enough to give a ratio pair with the desired properties. There are several numerical techniques for solving such equations, such as singular value decomposition or row reduction methods. A web site that features and explains the latter process is:
www.math.odu.edu/~bogacki/cgi-bin/lat.cgi?c=sys.

Incorporating Mineral Analyses in Pearce Element Diagrams

Pearce element ratios are often calculated for the stoichiometry of ideal mineral formulae or end members. The compositions of minerals actually sorted in rock-forming processes deviate to a greater or lesser extent from the compositions of end members. At best, these deviations will cause small amounts of scatter from the predicted trends on Pearce element ratio diagrams. At worst, they can produce significant deviations from the predicted trends.

Olivine and plagioclase are two commonly occurring minerals in mafic igneous rocks whose compositions are close enough to ideal to not cause scatter greater than analytical uncertainty. On the other hand, augite often contains Al, Ti,

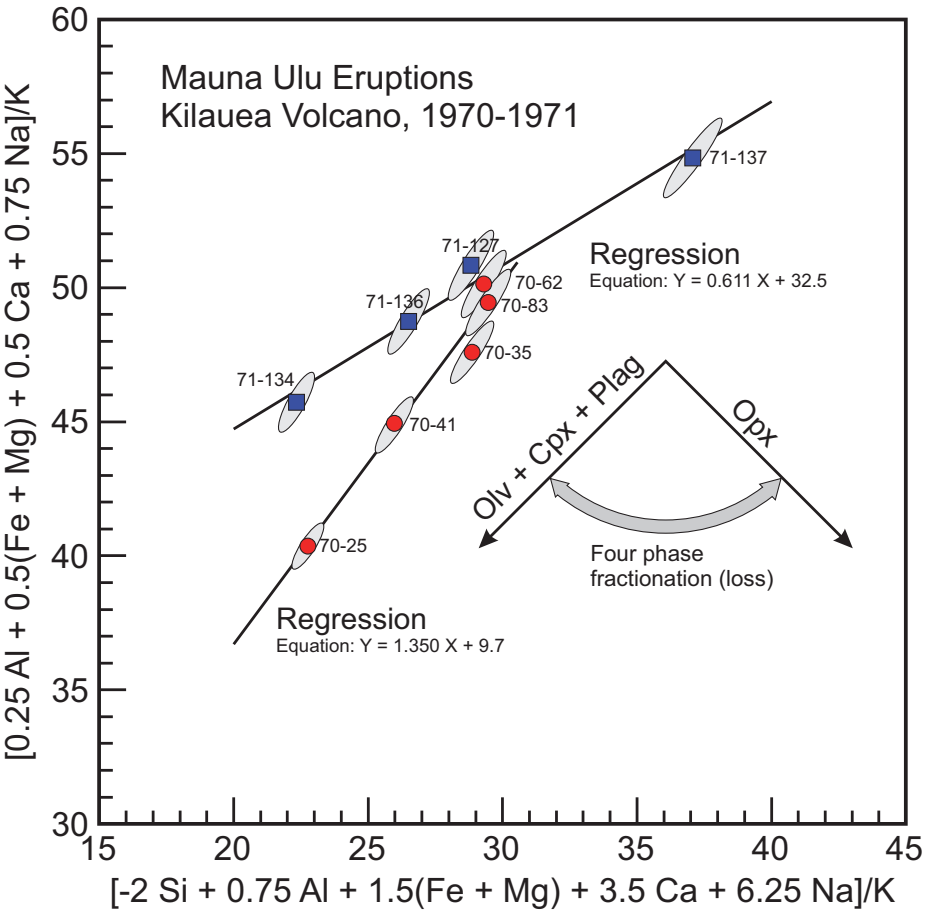

Figure 8. Phase discrimination diagram to best test whether sorting of orthopyroxene in addition to olivine, clinopyroxene, and plagioclase would affect the dispersion of the data compared to the diagrams in Figures 5, 6. The small arrows in the middle right contrast the trends successive melts would follow if fractionation of olivine, clinopyroxene, and plagioclase separated from the melts compared to separation of orthopyroxene. Separation of both olivine + plagioclase + clinopyroxene and orthopyroxene would create a trend between the two (broad grey arrow). The solid lines are the best fit, least-squares lines through the 1970 and 1971 data points. They approximate the paths in Pearce element ratio space that fractionation (all four phases, 1970 data) or accumulation (orthopyroxene) and fractionation (other three phases, 1971 data) would create. The tangents of the angles between the three-phase direction and the orthopyroxene directions are an estimate of the relative importance of the two processes, three-phase separation versus orthopyroxene separation or accumulation.

and excess Mg, deviating from the ideal. For some minerals, minor components can contribute substantial scatter to the data and a significant departure from the slope for an ideal end member. Table 4 lists the slopes expected from ideal solid solutions of olivine, plagioclase, and clinopyroxene and the analogous slopes calculated from analyses of typical basaltic minerals. The worst case is an error in slope of approximately 6° for an augite with considerable Al and Ti in solid solution.

Figure 9 shows two models testing whether the phase assemblage olivine, clinopyroxene, plagioclase, and an Fe-Ti oxide (Usp_{75}) can explain the chemical diversity in the 1967–1968 Halemaumau and Hi'iaka eruptions from Kilauea Volcano (Wright et al. 1975; Nicholls and Stout 1988). One model was constructed with an ideal clinopyroxene composition; the other was constructed using the composition of the most femic clinopyroxene-bearing sample (HI-14, Nicholls and Stout 1988, their table 4). The composition matrices (**C**, Eq. 1) are shown in Table 5. The entries in the Cpx row come directly from the formula calculated from the mineral analysis. The matrix methods described above return the same ratio for the X-axis for both models. Only the Y-axis ratio differs between the two models.

The foremost question is if the incorporation of an analyzed mineral composition provides more information on the adequacy of the model as an explanation for the chemical diversity? In this instance, the answer is no. Figure 9 shows that the data fit either model almost equally well. The data plotted with the two separate Y-axis coefficients (ideal solid solutions versus analyzed compositions) describe two lines that are different only in their Y-axis values. The two models describe linear trends of equal quality and allowing for real substitutions in the clinopyroxene do not improve the linearity nor do they reduce the dispersion in the location of the data points.

In other instances, incorporation of analyzed mineral compositions is essential for a successful Pearce element ratio analysis. If the sorted assemblage contains minerals of more variable stoichiometry, such as amphibole, then the deviations from the slopes expected for ideal compositions become more extreme. An innovative example is supplied by the data from the study of the granitic plutons forming part of the Coast Range Batholith in southwestern British Columbia (Cui and Russell 1995). They incorporated measured amphibole compositions into the phase composition matrices to create Pearce element ratio models for several different plutons that outcrop along a transect crossing the southwestern corner of the batholith. Intercepts revealed different source regions for different plutons, information not readily seen in the unmodified analytical data, indicating different chemical characteristics for source regions that supplied the granitic magma.

Verifying Pearce Element Ratio Diagrams

If, by some procedure or by inspiration one devises a ratio pair that is supposed to generate a trend with a slope dictated by a particular model; how, then, can the claim be verified? For example, how can one check that the pair of ratios plotted on Figure 4 will produce a slope of one if each of the phases in the model, olivine, plagioclase, and clinopyroxene, are sorted? This check becomes even more necessary if measured compositions of minerals in the samples are introduced into the phase composition matrix, **C** (Eq. 1, Table 5), or if the ratios come from inspiration. A diagram created through inspiration is shown on Figure 10. Neither sorting of plagioclase ($CaAl_2Si_2O_8$, $NaAlSi_3O_8$) nor clinopyroxene [$Ca(Mg,Fe)Si_2O_6$] will affect the distribution of data points on this diagram. It shows only the distribution caused by sorting of olivine [$(Mg,Fe)_2SiO_6$] and orthopyroxene [$(Mg,Fe)_2Si_2O_6$].

Fortunately, one can check for each phase that a diagram will produce a line with the slope dictated by the model. One

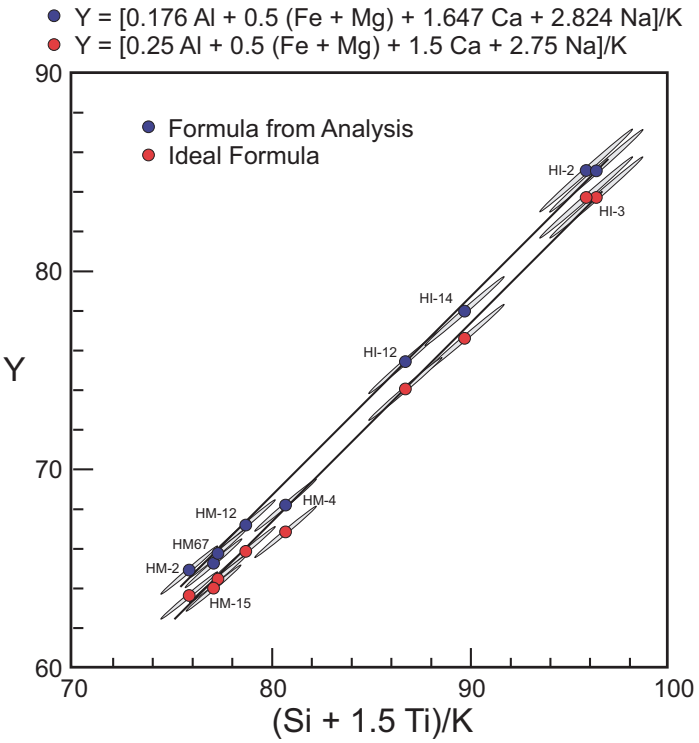

Figure 9. Two Pearce element ratio models to test whether the chemical diversity in the 1968 Kilauea eruptive products (Wright et al. 1975; Nicholls and Stout 1988) can be explained by sorting of olivine, clinopyroxene, plagioclase and Fe-Ti oxide (Usp_{75}). Lines with slopes of one are drawn through HI-3. The model shown in blue uses an analyzed pyroxene in the phase composition matrix (Eq. 1). The other model (shown in red) uses the ideal clinopyroxene formula [$Ca(Fe,Mg)\ Si_2O_6$].

does this by calculating the ratio of the components in the numerator of **Y** to those in the numerator of **X**. For the phase assemblage diagram (Fig. 4), the ratios are:

[0.25 Al + 0.5 (Fe + Mg) + 1.5 Ca + 2.75 Na]/K and Si/K

and the calculations that verify the ratios are:

$(Mg,Fe)_2SiO_4$ Olivine:	**Y**/**X** = [0.5 x 2 (Fe + Mg)]/1 Si = 1/1
$NaAlSi_3O_8$ Albite:	**Y**/**X** = [0.25 Al + 2.75 Na]/3 Si = 1/1
$CaAl_2Si_2O_8$ Anorthite:	**Y**/**X** = [0.25 x 2 Al + 1.5 Ca]/2 Si = 1/1
$Ca(Mg,Fe)Si_2O_6$ Cpx:	**Y**/**X** = [1.5 Ca + 0.5 Fe + Mg]/2 Si = 1/1

Given a mineral of known stoichiometry or composition, this procedure will return the slope of the trend that sorting of that phase will generate on the diagram. For example, on Figure 8, the arrows in the lower right corner show the directions loss of olivine, clinopyroxene, plagioclase, and orthopyroxene would impart to a trend caused by fractionation. Performing the exercise for orthopyroxene gives:

$(Mg,Fe)_2Si_2O_6$ Opx:

$$\mathbf{Y/X} = \tfrac{1}{2}[2(Fe + Mg)]/[-2(2Si)+1\tfrac{1}{2}\ 2(Fe + Mg)] = 1/-1$$

In other words, orthopyroxene sorting alone would generate a trend with a slope of –1.

Intercepts of Trends on Pearce Element Ratio Diagrams

Usually, geochemical trends are analyzed with regression methods and the trend is evaluated and interpreted on the basis of its slope, intercept, and the associated correlation coefficient. Pearce element ratio diagrams suggest an alternate strategy wherein the slope of the trend is dictated by the model. The slope is not extracted from the data; rather the model slope, representing a specific hypothesis, is compared directly against the data itself. Consequently, we can draw a line with the model slope through each data point on the diagram. Each data point will then define a unique intercept value. It is this set of intercepts that provides insight into the nature and uniqueness of the chemical system. Co-genetic rocks plotted on assemblage test diagrams ideally should have equal intercepts. In practice they will not because of analytical uncertainty. The intercepts will have a mean and a standard deviation consistent with the expected analytical uncertainties.

Significantly different intercepts in and between data sets distinguish different magma batches and, by inference, different melting events (Russell and Nicholls 1988; Russell and Stanley 1990a, b; Nicholls and Russell 1991; Cui and Russell 1995).

ORIGINS OF CHEMICAL VARIATIONS WITHIN THE 1970–1971 MAUNA ULU LAVA FLOWS

Our analysis of the geochemical compositions of the 1970 and 1971 Mauna Ulu lava flows with Pearce element ratios reveals several patterns and insights. First, the elements that are likely candidates for conserved behaviour in basaltic magmas show mixed results (Fig. 3). The data fall on a trend compatible with crystal sorting but with considerable scatter off the model trend (Fig. 4). Ratios of incompatible trace elements (Yb/Ce, Er/Ce, Dy/Ce, Eu/Ce, and Sm/Ce; Figs. 5, 6) separate the data into distinct sets that correlate with time of eruption.

Table 3 lists the values of the mean and variance for the ratios and intercepts for the full data set from the 1970–1971 Mauna Ulu eruptions. The values derive from the ratio pair used to create Figure 4:

[0.25 Al + 0.5 (Fe + Mg) + 1.5 Ca
+ 2.75 Na]/K versus Si/K

Also listed is the expected variation in the mean intercept values due to analytical uncertainty. The variation attributable to analytical uncertainty is less than the standard deviation of the data; a consequence expected if more than one chemical system is included in the data set (see Figs. 4, 5, 6). Three of the 1971 data points plot at values smaller or larger than the mean plus or minus the standard deviation whereas only one 1970 data point (70-25) has this distinction. Further, four of the five 1970 intercepts have values greater than the mean and three of the four 1971 data points have values less than the mean, again suggesting two magma batches.

Table 3 also lists the means and standard deviations for the ratios and intercepts for the two data groups separately, as delineated by the trace elements, along with the expected variations due to analytical uncertainty. The expected variation in analytical uncertainty for the 1970 samples is slightly larger than the standard deviation for the data. The 1971 data scatter considerably more than the expected analytical variation.

The question, therefore, is how to explain the chemical diversity expressed within and between the 1970 and 1971 Mauna Ulu lava flows? We consider four possible models:

Table 4. Comparison of slopes (*M*) calculated from mineral analyses to slopes for end members.

Ratio Pair	Mineral	*M* (Mineral Analysis)		*M* (Ideal Mineral)	
(**Fe** + **Mg**) vs. **Si**	Olivine	1.980 ± 0.033	63.2° ± 0.4°	2	63.4°
	Augite	0.638 ± 0.037	32.4° ± 1.5°	½	26.6°
(**2 Ca** + **Na**) vs. **Al**	Plagioclase	1.054 ± 0.015	46.4° ± 0.4°	1	45.0°
	Augite (N = 15)	13.473 ± 3.347	85.8° ± 1.2°	∞	90.0°

Table 5. Phase composition matrices for end member minerals and from a clinopyroxene calculated from a mineral analysis (Nicholls and Stout 1988).

End Member Matrix:

An	2	0	2	0	0	1	0
Ab	3	0	1	0	0	0	1
Fo	1	0	0	0	2	0	0
Fa	1	0	0	2	0	0	0
Di	2	0	0	0	1	1	0
Hd	2	0	0	1	0	1	0
Usp	0	0.75	0	2.25	0	0	0

Mineral Analysis Matrix:

An	2	0	2	0	0	1	0
Ab	3	0	1	0	0	0	1
Fo	1	0	0	0	2	0	0
Fa	1	0	0	2	0	0	0
Cpx	1.869	0.042	0.197	0.211	0.867	0.792	0.019
Usp	0	0.75	0	2.25	0	0	0

1. The chemical diversity of the Mauna Ulu samples arises through sorting of olivine, clinopyroxene, and plagioclase.
2. The diversity arises through sorting of the phenocryst phases combined with mixing of two chemically distinct magmas, the 1970 and the 1971 magma batches.
3. The diversity arises through sorting of olivine, clinopyroxene, and plagioclase plus another phase such as Fe-Ti oxide or orthopyroxene.
4. The diversity arises through melting of source regions with distinct differences in major element chemistry.

The 1970 and 1971 data sets define general trends expected from sorting olivine, clinopyroxene, and plagioclase (Model 1). However, in both cases, the dispersion in the Pearce element ratios is greater than can be ascribed to analytical uncertainties (Table 3). Consequently, we conclude that the scatter is too large for sorting to be the sole cause of the diversity, especially in the 1971 data. Although one could argue that the dispersion in the 1970 data is not large enough to definitely rule out the sorting model.

A model involving mixing between two magma batches represented by compositions within the 1970 and 1971 lava suites (Model 2) would be consistent with the major element dispersion shown on Figures 4 and 5. The end-member compositions involved in mixing could, for example, be the extreme compositions that fall on the extremes of the trends shown. The mixing model fails, however, because of the distinct separation in the trace element data between the 1970 and 1971 lava flows (Figs. 5, 6). If mixing occurred, the trace element ratios should show a dispersed pattern analogous to the dispersion of the major elements shown on Figure 4.

Model 3, which involves sorting of orthopyroxene, is questioned or rejected by many scientists because orthopyroxene has not been reported in any of the Mauna Ulu lava flows (Wright 1971; Wright and Fiske 1971; Wright et al. 1975; Hofmann et al. 1984). In fact, orthopyroxene phenocrysts are rarely found in recent Kilauea lava flows. The only exceptions among the modern eruptions are the lava flows erupted in 1955 (Ho and Garcia 1988), which contain orthopyroxene phenocrysts. It sporadically occurs in trace amounts in the groundmass of lava flows erupted on the flank of the volcano (Richter and Murata 1966). By contrast, lava flows erupted from neighbouring Mauna Loa typically contain orthopyroxene phenocrysts (Russell 1987). In some Mauna Loa flows they are overgrown by clinopyroxene (Nicholls and Stout 1997).

We view this problem from two perspectives: 1) Are there circumstances and conditions where orthopyroxene could be sorted and leave no physical indication of its presence but only a pattern in the chemical data? 2) Are there other tests for its participation?

To counter the rarity argument, one can consider thermodynamic modeling with MELTS (Ghiorso and Sack 1995). Such modeling shows that:

1. Basalt melts commonly have orthopyroxene as the first phase to crystallize with falling temperature at pressures corresponding to deeper parts of the Earth, depths below those of the mid-crust. Examples can be found in Russell (1987), Stout et al. (1989), Nicholls and Stout (1997), and Nicholls (2013). Figure 11 shows an example from the Mauna Ulu compositions. If sorting takes place at high pressure, say during transport, then it is conceivable that orthopyroxene would be part of the fractionated assemblage. At lower pressures, olivine and/or clinopyroxene and/or plagioclase crystallize first. If the melt is subjected to lower pressures on ascent and if the ascent rate is such that there is time for the orthopyroxene to dissolve, then no physical trace would remain. At the lower pressures, the high-pressure phases will be most out of equilibrium and the heat to dissolve them will come from the melt, lowering its temperature until the lower pressure phases (olivine and clinopyroxene) saturate again. The larger the pressure drop, the more the high-pressure phase is out of equilibrium, increasing the affinity for the dissolution reaction (Edwards and Russell 1996). The rate of dissolution increases with the affinity of reaction, increasing the likelihood that high-pressure phases will dissolve on ascent. Recent estimates of residence times in shallow magma reservoirs beneath Kilauea (30–200 years, Pietruszka and Garcia 1999) are times enough to dissolve early-formed orthopyroxene. The phase diagram on Figure 11 shows that a melt with the composition of the Mauna Ulu basalt 71-137 has this property.

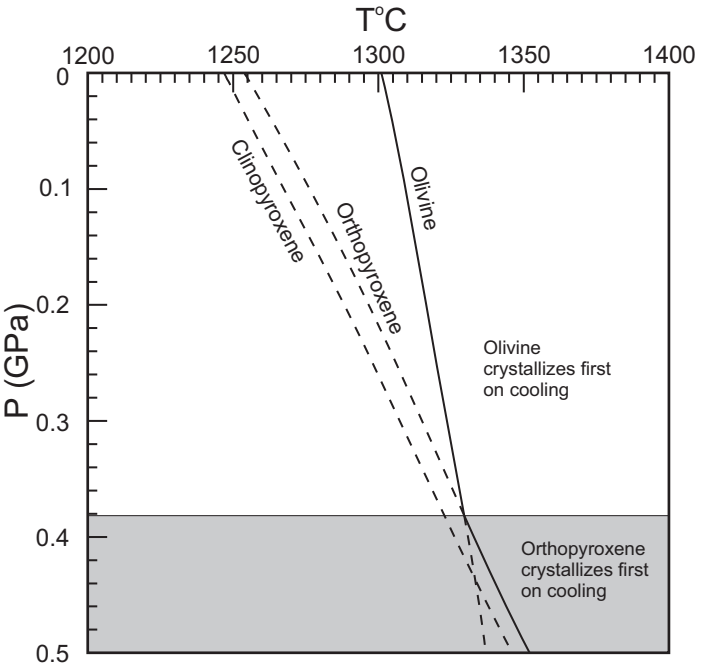

Figure 10. Pseudo-liquidus diagram computed for the bulk composition of a Mauna Ulu basalt 71-137 showing the curves of first saturation for the three phases: olivine, orthopyroxene, and clinopyroxene as a function of pressure and temperature. Curves calculated with MELTS (Ghiorso and Sack 1995). Curves are dashed where metastable.

2. Figure 8 shows the pattern expected for orthopyroxene sorting, although the data points for the 1970 data deviate little from the distribution expected for olivine, clinopyroxene, and plagioclase sorting (see Fig. 5). The variance expected from analytical uncertainty is slightly smaller than the variance in the data (Table 3). Another Pearce element ratio diagram is shown on Figure 10 that confirms the pattern shown by Figure 8: fractionation of orthopyroxene (and olivine) in the 1970 magmas and accumulation of orthopyroxene (and fractionation of olivine) in the 1971 magmas. Clinopyroxene and plagioclase sorting will produce no effect on the pattern displayed by the diagram (see Verifying Pearce Element Diagrams above).

For Model 4, chemical differences in the source regions, source processes, and chemically different source compositions provide the opportunity for creating chemical heterogeneity in magmas that are bound to have the chemical imprint of orthopyroxene (and other mantle mineralogy). The chemical diversity could arise from magma batches that result from different degrees of melting of the mantle source, or from incremental melting of the source, or from wall rock reaction attending transit through the overlying mantle. However, this model leaves little to be tested. Calls to coincidence to explain patterns will always provide the means for getting the pattern but such calls should be embraced only when all other explanations are totally inadequate.

THE LOGICAL STRUCTURE OF PEARCE ELEMENT RATIO DIAGRAMS

Pearce element ratio diagrams offer a rigorous and scientific means of testing our best ideas (i.e. models) concerning magmatic differentiation against geochemical data sets. Models are

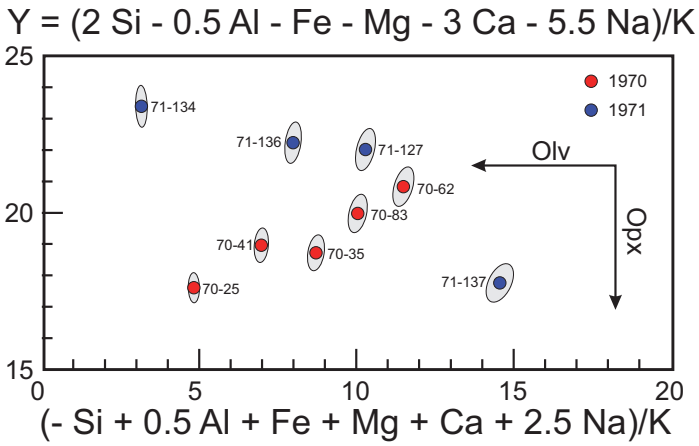

Figure 11. Pearce element ratio diagram that contrasts the pattern expected from olivine fractionation with the pattern expected from orthopyroxene fractionation. One can verify that plagioclase ($CaAl_2Si_2O_8$, $NaAlSi_3O_8$) and clinopyroxene [$Ca(Mg,Fe)Si_2O_6$] would produce a zero-length vector on the diagram. The arrows point in the direction fractionation (loss from system) would distribute data points.

propositions, constrained by logic, with testable consequences (Greenwood 1989). Pearce element ratio diagrams test the geochemical consequences of model ideas.

Models that are independent of the data are more powerful than those dependent on the data for their construction. In this regard, Pearce element ratio diagrams are ideal as they can be designed, independently of the geochemical data set, to represent specific models. For example, models of olivine sorting are expressed as a single straight line with a slope of 2 on a Pearce element ratio diagram of (Fe + Mg)/K versus Si/K (Fig. 1). The model can then be tested against the geochemical data. If the data are consistent with a single line of slope 2 the model is not rejected, and remains an adequate explanation of the variable olivine distributions within the lava flows and the geochemical data; otherwise the model is rejected.

It is over 40 years since publication of Pearce's original idea and over 25 years since a group of us put together a summary of how to use Pearce element ratio diagrams as petrologic tools (Russell and Stanley 1990). In that time there have been modifications and refinements to the paradigm (Russell et al. 1990) but the basic logical structures have remained the same. Consequently, we can confidently infer more about the 1970–1971 Mauna Ulu lava flows than we could in 1990. Dare we say that revisiting the same rocks in another twenty five years, possibly with additional data, would show even further improvement? We think so, which is what makes igneous petrology fun, satisfying, and, sometimes, frustrating.

ACKNOWLEDGEMENTS

We thank Jaroslav Dostal for inviting us contribute this paper to Geoscience Canada. We acknowledge and thank Cindy Murphy and Rob Raeside for their significant editorial contributions and two anonymous reviewers who told us the first submission was not good enough and do it again. They were right.

REFERENCES

Ayres, F., Jr., 1962, Theories and problems of matrices: McGraw-Hill Book Company, New York.

Beswick, A.E., 2002, An analysis of compositional variations and spatial relationships within Fe–Ni–Cu sulfide deposits on the North Range of the Sudbury Igneous Complex: Economic Geology, v. 97, p. 1487–1508, http://dx.doi.org/10.2113/97.7.1487.

Beswick, A.E., 2013, Some applications of element ratio analysis to understanding the compositional variations displayed by a selection of Fe–Ni–Cu–PGE deposits at Sudbury, Ontario, Canada (Poster): Proceedings 36th Annual Winter Meeting of the Geological Society's Mineral Deposits Studies Group, University of Leicester, UK.

Cui, Y., and Russell, J.K., 1995, Magmatic origins of calc-alkaline intrusions from the Coast Plutonic Complex, southwestern British Columbia: Canadian Journal of Earth Sciences, v. 32, p. 1643–1667, http://dx.doi.org/10.1139/e95-131.

Deer, W.A., Howie, R.A., and Zussman, J., 2013, An introduction to the rock-forming minerals (3rd edition): Mineralogical Society, London, 498 p.

Edwards, B.R., and Russell, J.K., 1996, A review and analysis of silicate mineral dissolution experiments in natural silicate melts: Chemical Geology, v. 130, p. 233–245.

Ghiorso, M.S., and Sack, R.O., 1995, Chemical mass transfer in magmatic processes IV. A revised and internally consistent thermodynamic model for the interpolation and extrapolation of liquid-solid equilibria in magmatic systems at elevated temperatures and pressures: Contributions to Mineralogy and Petrology, v. 119, p. 197–212, http://dx.doi.org/10.1007/BF00307281.

Greenwood, H.J., 1989, On models and modeling: Canadian Mineralogist, v. 27, p. 1–14.

Halleran, A.D., and Russell, J.K., 1990, Trace elements formulated as Pearce element ratios. II. Recognition of open system behavior, *in* Russell, J.K., and Stanley, C.R., *eds.*, Theory and Application of Pearce Element Ratios to Geochemical Data Analysis, Volume 8: Geological Association of Canada, Vancouver, BC, p. 243–270.

Ho, R.A., and Garcia, M.O., 1988, Origin of differentiated lavas at Kilauea Volcano, Hawaii: Implications from the 1955 eruption: Bulletin of Volcanology, v. 50, p. 35–46, http://dx.doi.org/10.1007/BF01047507.

Hofmann, A.W., Feigenson, M.D., and Raczek, I., 1984, Case studies on the origin of basalt: III. Petrogenesis of the Mauna Ulu eruption, Kilauea, 1969–1971: Contributions to Mineralogy and Petrology, v. 88, p. 24–35, http://dx.doi.org/10.1007/BF00371409.

Nicholls, J., 1988, The statistics of Pearce element diagrams and the Chayes closure problem: Contributions to Mineralogy and Petrology, v. 99, p. 11–24, http://dx.doi.org/10.1007/BF00399361.

Nicholls, J., 1990, Stochiometric constraints on variations in Pearce element ratios and analytical uncertainty in hypothesis testing, *in* Russell, J.K., and Stanley, C.R., *eds.*, Theory and Application of Pearce Element Ratios to Geochemical Data Analysis, Volume 8: Geological Association of Canada, Vancouver, BC, p. 73–98.

Nicholls, J., 2013, Perfect fractionation in multicomponent, multiphase systems: Contributions to Mineralogy and Petrology, v. 166, p. 691–701, http://dx.doi.org/10.1007/s00410-013-0897-y.

Nicholls, J., and Gordon, T.M., 1994, Procedures for the calculation of axial ratios on Pearce element-ratio diagrams: Canadian Mineralogist, v. 32, p. 969–977.

Nicholls, J., and Russell, J.K., 1990, Pearce element ratios - An overview, example and bibliography, *in* Russell, J.K., and Stanley, C.R., *eds.*, Theory and Application of Pearce Element Ratios to Geochemical Data Analysis, Volume 8: Geological Association of Canada, Vancouver, BC, p. 11–21.

Nicholls, J., and Russell, J.K., 1991, Major-element chemical discrimination of magma batches in lavas from Kilauea volcano, Hawaii, 1954–1971 eruptions: Canadian Mineralogist, v. 29, p. 61–74.

Nicholls, J., and Stout, M.Z., 1988, Picritic melts in Kilauea — Evidence from the 1967–1968 Halemaumau and Hiiaka eruptions: Journal of Petrology, v. 29, p. 1031–1057, http://dx.doi.org/10.1093/petrology/29.5.1031.

Nicholls, J., and Stout, M.Z., 1997, Epitactic overgrowths and intergrowths of clinopyroxene on orthopyroxene: Implications for paths of crystallization, 1881 lava flow, Mauna Loa Volcano, Hawaii: Canadian Mineralogist, v. 35, p. 909–922.

Oviatt, C.G., and Nash, W.P., 1989, Late Pleistocene basaltic ash and volcanic eruptions in the Bonneville basin, Utah: Geological Society of America Bulletin, v. 101, p. 292–303, http://dx.doi.org/10.1130/0016-7606(1989)101<0292:LPBAAV>2.3.CO;2.

Pearce, T.H., 1968, A contribution to the theory of variation diagrams: Contributions to Mineralogy and Petrology, v. 19, p. 142–157, http://dx.doi.org/10.1007/BF00635485.

Pietruszka, A.J., and Garcia, M.O., 1999, The size and shape of Kilauea Volcano's summit magma storage reservoir: a geochemical probe: Earth and Planetary Science Letters, v. 167, p. 311–320, http://dx.doi.org/10.1016/S0012-821X(99)00036-9.

Press, W.H., Teukolsky, S.A., Vetterling, W.T., and Flannery, B.P., 1992, Numerical recipes in FORTRAN: The art of scientific computing: Cambridge University Press, Cambridge, England, 963 p.

Richter, D.H., and Murata, K.J., 1966, Petrography of the lavas of the 1959–60 eruption of Kilauea Volcano, Hawaii: U.S.G.S Professional Paper, 537-D, Washington, DC, p. 1–14.

Russell, J.K., 1987, Crystallization vesiculation of the 1984 eruption of Mauna Loa: Journal of Geophysical Research, v. 92, p. 13731–13743, http://dx.doi.org/10.1029/JB092iB13p13731.

Russell, J.K., and Halleran, A.D., 1990, Trace elements formulated as Pearce element ratios II: Recognition of open system behaviour, *in* Russell, J.K., and Stanley, C.R., *eds.*, Theory and Application of Pearce Element Ratios to Geochemical Data Analysis, Volume 8: Geological Association of Canada, Vancouver, BC, p. 55–72.

Russell, J.K., and Nicholls, J., 1988, Analysis of petrologic hypotheses with Pearce element ratios: Contributions to Mineralogy and Petrology, v. 99, p. 25–35, http://dx.doi.org/10.1007/BF00399362.

Russell, J.K., and Stanley, C.R., 1990a, Origins of the 1954–1960 lavas, Kilauea Volcano, Hawaii: Major element constraints on shallow reservoir magmatic processes: Journal of Geophysical Research, v. 95, p. 5021–5047, http://dx.doi.org/10.1029/JB095iB04p05021.

Russell, J.K., and Stanley, C.R., 1990b, Theory and application of Pearce Element Ratios to geochemical data analysis: Geological Association of Canada, Short Course Notes, v. 8, Vancouver, BC, p. 315.

Russell, J.K., Nicholls, J., Stanley, C.R., and Pearce, T.H., 1990, Pearce element ratios: A paradigm for testing hypotheses: Eos, v. 71, p. 234–236, 246–247.

Stanley, C.R., 1993, Effects of non-conserved denominators on Pearce element ratio diagrams: Mathematical Geology, v. 25, p. 1049–1070, http://dx.doi.org/10.1007/BF00911549.

Stanley, C.R., 2003, Estimating sampling errors for major and trace elements in geological materials using a propagation of variance approach: Geochemistry: Exploration, Environment, Analysis, v. 3, p. 169–178, http://dx.doi.org/10.1144/1467-7873/03-008.

Stanley, C.R., 2006a, Numerical transformation of geochemical data: 1. Maximizing geochemical contrast to facilitate information extraction and improve data presentation: Geochemistry: Exploration, Environment, Analysis, v. 6, p. 69–78, http://dx.doi.org/10.1144/1467-7873/05-078.

Stanley, C.R., 2006b, Numerical transformation of geochemical data: 2. Stabilizing measurement error to facilitate data interpretation: Geochemistry: Exploration, Environment, Analysis, v. 6, p. 79–96, http://dx.doi.org/10.1144/1467-7873/05-079.

Stanley, C.R., and Madeisky, H.E., 1995, Pearce Element Ratio analysis in lithogeochemical exploration: 17th International Geochemical Exploration Symposium Association of Exploration Geochemists, Annual Meeting, Short Course, Townsville, Queensland, Australia, 96 p.

Stanley, C.R., and Russell, J.K., 1989, Petrologic hypothesis testing with Pearce element ratio diagrams: Derivation of diagram axes: Contributions to Mineralogy and Petrology, v. 103, p. 78–89, http://dx.doi.org/10.1007/BF00371366.

Stanley, C.R., and Russell, J.K., 1990, Matrix methods for the development of Pearce element ratio diagrams, *in* Russell, J.K., and Stanley, C.R., *eds.*, Theory and Application of Pearce Element Ratios to Geochemical Data Analysis, Volume 8: Geological Association of Canada, Vancouver, BC, p. 1311–1156.

Stout, M.Z., Nicholls, J., and Kuntz, M.A., 1989, Fractionation and contamination processes, Craters of the Moon Lava Field, Idaho, 2000–2500 years BP: Bulletin New Mexico Bureau of Mines & Mineral Resources, v. 131, p. 259.

Vinet, N., and Higgins, M.D., 2010, Magma solidification processes beneath Kilauea Volcano, Hawaii: a quantitative textural and geochemical study of the 1969–1974 Mauna Ulu lavas: Journal of Petrology, v. 51, p. 1297–1332, http://dx.doi.org/10.1093/petrology/egq020.

Wright, T.L., 1971, Chemistry of Kilauea and Mauna Loa in space and time: U.S.G.S. Professional Paper, 735, p. 1–40.

Wright, T.L., and Fiske, R.S., 1971, Origin of the differentiated and hybrid lavas of Kilauea Volcano, Hawaii: Journal of Petrology, v. 12, p. 1–65, http://dx.doi.org/10.1093/petrology/12.1.1.

Wright, T.L., Swanson, D.A., and Duffield, W.A., 1975, Chemical compositions of Kilauea east-rift lava, 1968–1971: Journal of Petrology, v. 16, p. 110–133, http://dx.doi.org/10.1093/petrology/16.1.110.

Received March 2015
Accepted as revised January 2016
First published on the web February 2016

Access to the Excel spreadsheet of the Pearce element ratio program is available through the GAC's Geoscience Canada Data Repository, Igneous Rock Associations series link at: http://www.gac.ca/wp/?page_id=12081.